RSC Advances

This is an *Accepted Manuscript*, which has been through the Royal Society of Chemistry peer review process and has been accepted for publication.

Accepted Manuscripts are published online shortly after acceptance, before technical editing, formatting and proof reading. Using this free service, authors can make their results available to the community, in citable form, before we publish the edited article. This *Accepted Manuscript* will be replaced by the edited, formatted and paginated article as soon as this is available.

You can find more information about *Accepted Manuscripts* in the **Information for Authors**.

ROYAL SOCIETY OF CHEMISTRY

www.rsc.org/advances

Journal Name

COMMUNICATION

Microdomain Orientation Control of PS-*b*-PMMA Film Enabled by Wettability Relay of Graphene

Mei-Ling Wu[ab] and Dong Wang*[a]

Orientation control of block copolymer (BCP) microdomains in thin film is an important step for robust pattern transfer in BCP-based nanolithography. The established orientation control of BCP film relies on neutral surface modification using random copolymer brush covalently bonded to substrates with proper anchoring groups, which is limited to specific substrates. Herein, we reported utilizing monolayer graphene to physically separate neutral random copolymer layer and BCP film, and at the same time, relay the wettability of neutral interface to achieve a perpendicularly oriented control of self-assembly of PS-*b*-PMMA microdomains. We demonstrate that the method is widely applicable to achieve the orientation control of the BCP film on various substrates.

1. Introduction

Block copolymer (BCP) can spontaneously self-assemble into dense periodic arrays in a scalable manner with feature size in the range of 10-100 nm.[1] The self-assembled BCP thin film can act as a template to control over the spatial order of other materials by taking advantage of the chemical or physical property difference of the BCP blocks.[2-4] BCP-based nanopatterning technique is known for tunable and nanoscale scale feature size, high throughput, low cost, and favorable compatibility with current nanolithography techniques,[5-7] and has attracted considerable attention in many fields, such as microelectronic device,[8] nano chemical reactor,[9] magnetic storage,[10] et al.[11-13]

The free energy of substrate plays a critical role in tuning the morphology of BCP thin films.[14] Generally, perpendicular orientation of BCP film is more desirable as it can facilitate robust pattern transfer.[15, 16] Neutral surface modification is usually utilized to balance the interfacial energies of both components towards substrates to achieve a perpendicularly

orientated BCP film.[14] So far, various surface modification approaches for this purpose have been developed based on copolymer brush and mat,[17, 18] self-assembled monolayer,[19] and other surface treatment methods.[3, 20, 21] For example, random copolymer brush, i.e., hydroxyl ended PS-*r*-PMMA (PS-*r*-PMMA-OH), is recognized as a simple and effective way to control the microdomain orientation of PS-*b*-PMMA.[22-25] However, the copolymer brush must be covalently bonded with the substrate through anchoring hydroxyl groups so as not to diffuse into the BCP films during the thermal annealing, becoming a preferential surface.[17, 18] Therefore, random copolymer brush is generally suitable for substrates with native hydroxyl groups (such as silicon oxide)[3, 26] or substrates after active oxygen treatment, such as Au treated by oxygen plasma.[21] Although oxygen plasma is effective to achieve active oxygen functional groups on some substrates, it is unsuitable for polymer substrates (such as polyimide) and the treating condition depends on specific substrate. To overcome the substrate dependence of random copolymer brush for BCP self-assembly, some substrate-independent methods such as free-standing BCP film,[20, 27] polymer mat[18] have been developed to extend the range of applicable surfaces and substrates for BCP nanolithography.

Here, we demonstrate that the PS-*b*-PMMA film can form a perpendicularly oriented microdomain by using monolayer graphene as a mediator layer between the random PS-*r*-PMMA layer and PS-*b*-PMMA film. Graphene is an atomically thin two-dimensional material that possesses excellent mechanical strength,[28] and has been applied in BCP-based nanopatterning technique as a favorable substrate, surface energy modifier, and support for free-standing BCP film.[13, 20, 29] In this study, we prove that graphene can act as a barrier interlayer that prevents the random copolymer from diffusing into the BCP layer. On the other hand, the atom-thick graphene is considered as a transparent film for some surface properties and can relay the interfacial energy of the random copolymer to BCP thin film.[30-32] This method eliminates the necessity of end-functionalized hydroxyl group to anchor the substrate, and is therefore applicable to a wide range of substrates.

a. Key Laboratory of Molecular Nanostructure and Nanotechnology and Beijing National Laboratory for Molecular Sciences, Institute of Chemistry, Chinese Academy of Sciences (CAS), Beijing 100190, P. R. China.
E-mail：wangd@iccas.ac.cn.
b. University of CAS, Beijing 100049, P. R. China.

RSC Advances Accepted Manuscript

2. Experimental Section

Materials. Random copolymer composed of styrene and methylmethacrylate (PS-*r*-PMMA; molecular weight, 14k g mol^{-1}; PS volume fraction, 58%), hydroxyl-terminated PS-*r*-PMMA (molecular weight, 14.3k g mol^{-1}; PS volume fraction, 56%) and diblock copolymers (PS-*b*-PMMA) were purchased from Polymer Source. Si wafer was cleaned with piranha solution. Thin layers of Au, Cu, Mo films were deposited on Si wafer by magnetron sputtering (PVD75, Kurt J. Lesker).

Deposition of random copolymer films. PS-*r*-PMMA random copolymer with a PS friction of 58% was dissolved in toluene (1-2 mg ml^{-1}) and spin-coated on substrates. The substrates with random copolymer were baked at 120 °C for 5 min to remove the residual toluene. PS-*r*-PMMA-OH was dissolved in toluene (5 mg ml^{-1}) and spin-coated on SiO$_2$ substrate. The substrate with PS-*r*-PMMA-OH film was then thermal annealed at 230 °C for 5 h under Ar flow. Unanchored PS-*r*-PMMA-OH film was washed away by toluene solution in ultrasonic bath.

Graphene synthesis and transfer. Monolayer graphene was synthesized on copper foil by the chemical vapor deposition method as described in previous papers.[20, 33] Briefly, a clean copper coil (25 μm) was first annealed at 1000 °C under a H$_2$/Ar flow, and further treated with a mix atmosphere of CH$_4$, H$_2$, and Ar at 1050 °C for 1 h to form monolayer graphene. The graphene was then transferred onto random copolymer film using a dry-transfer method with a polydimethylsiloxane (PDMS) stamp.[34] After the graphene was transferred onto substrates coated by PS-*r*-PMMA, it was baked at 120 °C for 10 min and then dried *in vacuo* for 30 min to increase the interaction force between the graphene and substrate.

Self-assembly of PS-*b*-PMMA film. Cylinder-forming PS-*b*-PMMA (46k-21k) and lamella-forming PS-*b*-PMMA (53k-54k) diblock copolymers were dissolved in toluene to form solution of 11 mg mL^{-1} and 15 mg mL^{-1}, respectively, and were spin-coated onto the graphene coated random film to form thin films. The film thicknesses were 52 and 77 nm, respectively, according to the spectroscopic ellipsometer (SE 850 DUV, SENTECH Instruments). The BCP films were annealed at 250 °C in Ar for 24 h for sufficient microphase separation. For the scanning electron microscopy (SEM) observation, PMMA domains of BCP samples were removed selectively with Ar plasma with a 50 sccm Ar flow rate and radio frequency power of 30 W.

Characterization. The surface morphology of self-assembled BCP film was observed on Helios 600i SEM with a field emission source of 5 kV *in vacuo* (< 10^{-4} mbar). Raman spectra and mappings of graphene were collected with a Microscope Raman Spectroscopy (Thermo Scientific DXR) motivated by a laser of 532 nm. Atomic force microscopy (AFM, Multimode 8, Vecoo) was operated in the tapping mode using silicon probe tip. Water contact angle was measured with optical contact angle measuring device (DSA 100, KRUSS).

3. Results and Discussion

Graphene Mediated Orientation Control of PS-*b*-PMMA.

The overall process to fabricate the perpendicularly orientated PS-*b*-PMMA film is schematically presented in Fig. 1. Briefly, a PS-*r*-PMMA film (film thickness, ~5 nm) was first spin-coated on a substrate. After that, graphene grown by chemical vapor deposition was carefully transferred onto it. PS-*b*-PMMA film was then spin-coated on the graphene surface and thermal-annealed for microphase separation, during which cylinder or lamellar microdomain orientates normal to the substrate as a result of minimum interfacial energy. To facilitate observation for the BCP self-assembled morphology by SEM, the self-assembled BCP film was exposed to Ar plasma to selectively remove the PMMA blocks.
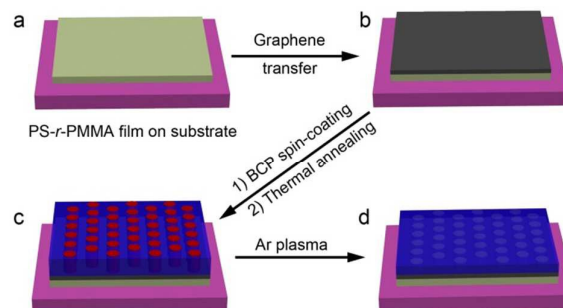
Fig. 1 Schematic of fabrication of a perpendicularly orientated PS-*b*-PMMA film with graphene coated random film (taking cylinder-forming PS-*b*-PMMA as an example).

The quality of the graphene transferred on PS-*r*-PMMA film is examined by Raman spectra. In the Raman spectra of graphene coated PS-*r*-PMMA film, Raman signal of PS-*r*-PMMA film was too weak to be detected. The single-point Raman spectrum (Fig. 2a) exhibits the G peak (1580 cm^{-1}) and 2D peak (2680 cm^{-1}), which are the characteristic peaks of graphene. The intensity ratio of 2D band to G band (I_{2D}/I_G) is approximately 2.0, indicating a monolayer graphene. D peak (1350 cm^{-1}) of graphene, which is attributed to the defects of graphene, is weakly detected, suggesting that the transferred graphene is of high quality with negligible defects. To demonstrate that the graphene is coated uniformly and integrally across the surface of the PS-*r*-PMMA brush, we further preformed Raman mapping of the graphene film over large area. Intensity ratios, I_{2D}/I_G and I_D/I_G, are depicted in the color contour plots in Figs. 2b and 2c. It is evident that the transferred graphene film has uniform I_{2D}/I_G (~2.0) with low I_D/I_G (0-0.2) across the whole area, indicating an integrated monolayer graphene. Furthermore, we utilized AFM to reveal the morphology of the graphene on the PS-*r*-PMMA film. The topology of PS-*r*-PMMA brush on Si wafer is shown in Fig. 2d. With graphene transferred on the brush (Fig. 2e), a uniform morphology is obtained, representing the typical morphology of graphene films. Sporadic wrinkles and contaminations are found in Fig 2e, which mainly resulted from the growth and transfer process of graphene. The Raman spectra and AFM images demonstrate that the integrated and uniform monolayer graphene is successfully and conformably coated on the random copolymer film and is ready for the subsequent processes.
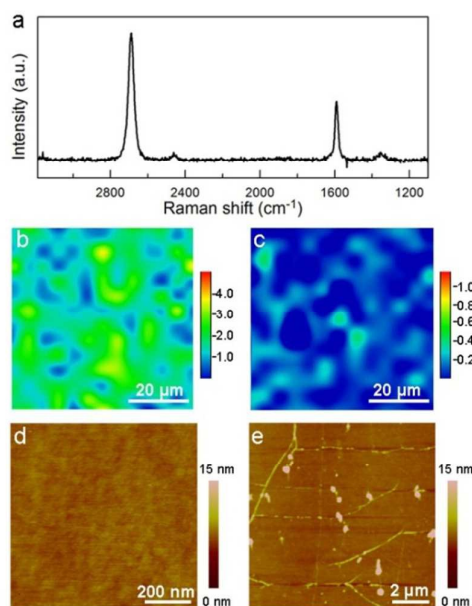
Fig. 2 (a) Raman spectra of graphene transferred onto PS-*r*-PMMA film, and its corresponding contour plot of Raman peak intensity ratio: (b) I_{2D}/I_G, (c) I_D/I_G; AFM height image of (d) PS-*r*-PMMA film; (e) graphene coated PS-*r*-PMMA film.


Fig. 3 Schematic structure (a, d), planar view (b, e) and side view (52°) (c, f) SEM images of lamella-forming (upper row) and cylinder-forming (lower row) PS-*b*-PMMA morphology self-assembled on graphene coated random film. Corresponding large-area PS-*b*-PMMA films are shown in insets.

The cylinder and lamella types of PS-*b*-PMMA (depending on molecular weight ratio of each block) were spin-coated on the graphene coated random copolymer layer on the SiO_2 substrate and thermally annealed afterwards. The film thicknesses of cylinder-forming and lamella-forming PS-*b*-PMMA films are approximately 1.4 L_0 (L_0 = 36 nm for cylinder-forming BCP and 56 nm for lamella-forming BCP, measured from the SEM images). For the lamella-forming PS-*b*-PMMA, fingerprint array indicates the formation of perpendicularly oriented lamella domains; for the cylinder-forming PS-*b*-PMMA, hexagonal array is expected. Fig. 3 depicts the scheme and self-assembled morphologies of PS-*b*-PMMAs on graphene coated random film after PMMA block removal. Based on the planar-view and side-view SEM images, well-defined fingerprint arrays of PS(53k)-*b*-PMMA(54k) (Figs. 3b and 3c) are formed, which indicate that a perpendicular lamella is achieved. Hexagonal arrays of PS(46k)-*b*-PMMA(21k) (Figs. 3e and 3f) indicate that perpendicularly oriented cylinder domains are also formed on graphene with an underlying random copolymer layer. Moreover, the uniformly self-assembled BCP film with perpendicular orientation can be easily achieved in a large area (indicated by the uniform contrast of the large-area SEM image in the insets in Figs. 3b and 3e). These results demonstrate that the orientational control of PS-*b*-PMMA is feasible mediated by graphene coated random copolymer layer.

Orientation Control on Different Substrates.
The approach using graphene coated PS-*r*-PMMA eliminates the necessity of end-functionalized hydroxyl group to anchor the substrate, and is thus expected to be a method independent of the substrate. To substantiate the applicability of this method,
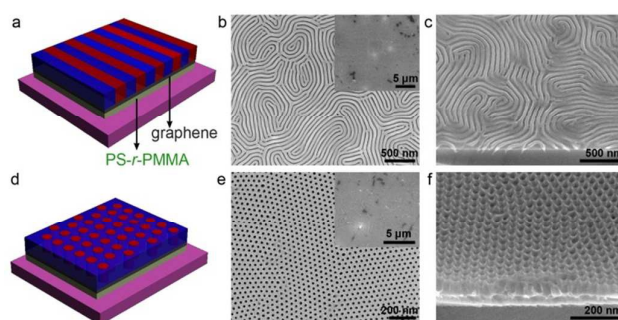
orientation control of BCP film based on graphene coated PS-*r*-PMMA layer was realized on various substrates aside from SiO_2, including Au, Cu, Mo, and polyimide (PI). As shown in Fig. 4a, we can easily fabricate PS-*b*-PMMA nanopattern on the Au substrate with graphene interlayer coated random copolymer layer. From the side view SEM image of nanopattern on Si wafer in Fig. 4a, we can clearly observe the Au layer on Si wafer, graphene, and the ordered hexagonal arrays of PS(46k)-*b*-PMMA(21k) film. Similarly, employing the graphene coated random film as a mediated layer, perpendicular BCP cylinder nanopatterns could also be successfully fabricated on Si, Cu, Mo, and PI substrates (Figs. 4b-f).

Mechanism Insight on the Role of Graphene.
The effect of graphene on the random copolymer in BCP self-assembly is investigated. As shown in Fig. 5, PS-*r*-PMMA film (note that the random copolymer contains no hydroxyl groups) was partially covered by graphene film, on which PS-*b*-PMMA was subjected to thermally driven self-assembly. From the optical microscope image and corresponding Raman mapping (contour plot of 2D band intensity) of self-assembled BCP film with underlying graphene and PS-*r*-PMMA film shown in Figs. 5a and 5b, we can clearly see that half area of PS-*r*-PMMA film is coated with graphene. The morphology of subsequently self-assembled PS-*b*-PMMA film was observed by SEM (Figs. 5c-e). The striking contrast of the BCP morphologies on the
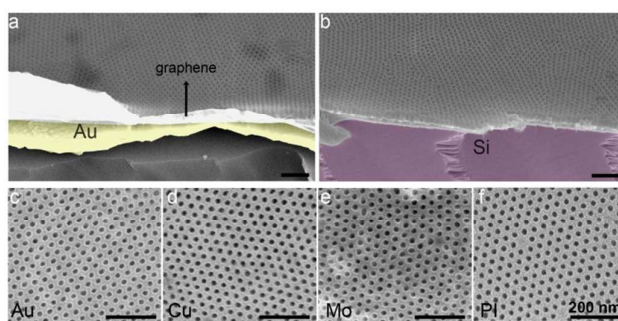

Fig. 4 SEM images of cylinder-forming PS-*b*-PMMA on various substrates: (a, b) side view (52°); (c-f) planar view.
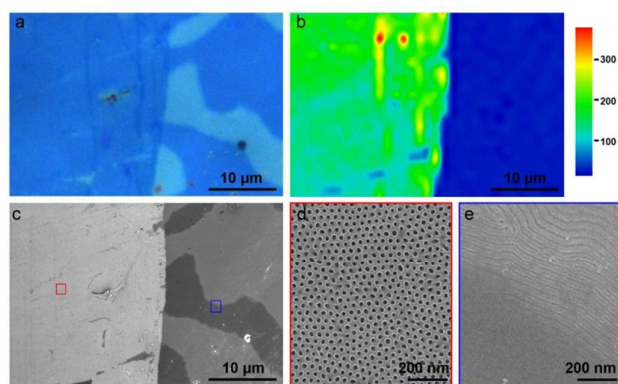
Fig. 5 Self-assembled PS(46k)-*b*-PMMA(21k) film on a PS-*r*-PMMA film partly coated by graphene: (a) optical microscope image, (b) corresponding scanning Raman mapping of 2D band of graphene, (c) SEM image, (d) high-magnified SEM image in the red rectangle of (c), (e) the high-magnified SEM image in the blue rectangle of (c).

Fig. 6 SEM images of lamella-forming PS(53k)-*b*-PMMA(54k) on substrates modified by different layers (illustrated above the SEM images): (a) PS-*r*-PMMA-OH, (b) PS-*r*-PMMA, (c) graphene.

graphene coated PS-*r*-PMMA film (Fig. 5d) and the bare PS-*r*-PMMA film (Fig. 5e), that is, perpendicular orientation in the former and parallel orientation in the latter, unambiguously validate the effect of graphene interlayer on the BCP self-assembly.

Further control experiments were conducted to understand the principle of PS-*b*-PMMA self-assembly on the graphene coated random copolymer film. We first employed the hydroxyl ended PS-*r*-PMMA-OH on SiO_2 for the self-assembly of PS(53k)-*b*-PMMA(54k). Perpendicularly oriented microdomain is formed with fingerprint arrays as expected (Fig. 6a), which verifies its well-known effect of providing a neutral surface for the orientation control of PS-*b*-PMMA film. This morphology is very similar to that in Fig. 3b, in which graphene coated random copolymer film is the substrate, indicating that the graphene relays the neutral wettability of random copolymer. This is evidenced by the contact angle of water on graphene coated random polymer film, which is 74.4° ± 2.3°, close to that on neutral surfaces in several papers.[20, 25, 29] Thus, the random copolymer film coated with graphene remains a neutral surface. When we use the PS-*r*-PMMA without hydroxyl end groups to control the orientation of PS(53k)-*b*-PMMA(54k) film, however, featureless morphology is obtained (Fig. 6b, parallel orientation), because PS-*r*-PMMA without hydroxyl groups cannot be anchored on the SiO_2 surface and would diffuse into the BCP film during thermal annealing.[17] The failure to control the orientation of BCP film on PS-*r*-PMMA film indicates that substrate anchor or physical barrier is necessary to prevent random copolymer diffusion. When PS-*r*-PMMA is coated with graphene film, PS-*b*-PMMA film can easily self-assemble on the graphene coated PS-*r*-PMMA film with perpendicular orientation (Fig. 3). As the PS-*r*-PMMA is not bonded on the substrate, it is the graphene interlayer that prevents the PS-*r*-PMMA from diffusing into the BCP film. This function is somewhat similar to that with hydroxyl end groups but it no longer depends on the substrate. In addition, as shown in Fig. 6c, PS-*b*-PMMA film cannot form perpendicular orientation on
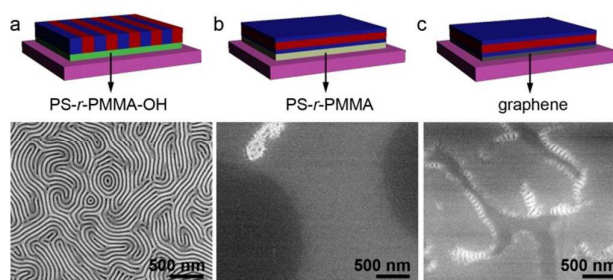
graphene surface, because of the low surface energy of graphene.[20] Therefore, the self-assembly of perpendicularly oriented BCP film is still attributed to the effect of neutral surface of random copolymer. The graphene acts as an integrate and mechanically strong interlayer that prevents PS-*r*-PMMA from diffusing into the BCP film, and on the other hand, it is a wetting transparent (or translucent) interlayer that can relay the wettability of PS-*r*-PMMA film to orientate the BCP film even physically separated by graphene (because of the atom-scale thickness of graphene).[30, 31]

4. Conclusions

In summary, we demonstrated a new method to control the orientation of PS-*b*-PMMA film mediated by graphene coated PS-*r*-PMMA random layer. This method is proved to be an effective way to achieve perpendicularly oriented microdomain of PS-*b*-PMMA film on various substrates. We demonstrate that the broad applicability of this method to substrate with different surface functionalities is attributed to dispensing PS-*r*-PMMA film from linking to the substrates through anchoring groups. The graphene acts as not only a resist layer to keep the PS-*r*-PMMA from diffusing into the BCP layer, but also a quasi-transparent layer that can relay the wettability of underlying PS-*r*-PMMA film to the BCP film. The proposed method is promising to offer an alternative approach for BCP-based lithography and also provide a potentially simple and non-destructive way to fabricate monolayer graphene nanopatterns.

Acknowledgement

References

1   M. Park, C. Harrison, P. M. Chaikin, R. A. Register and D. H. Adamson, *Science*, 1997, **276**, 1401-1404.
2   J. Bang, U. Jeong, Y. Ryu du, T. P. Russell and C. J. Hawker, *Adv. Mater.*, 2009, **21**, 4769-4792.

3 S.-J. Jeong, G. Xia, B. H. Kim, D. O. Shin, S.-H. Kwon, S.-W. Kang and S. O. Kim, *Adv. Mater.*, 2008, **20**, 1898-1904.

4 P. Bai, J. Kao, J. H. Chen, W. Mickelson, A. Zettl and T. Xu, *Nanoscale*, 2014, **6**, 4503-4507.

5 J. Chai, D. Wang, X. Fan and J. M. Buriak, *Nat. Nanotechnol.*, 2007, **2**, 500-506.

6 J. K. Yang, Y. S. Jung, J. B. Chang, R. A. Mickiewicz, A. Alexander-Katz, C. A. Ross and K. K. Berggren, *Nat. Nanotechnol.*, 2010, **5**, 256-260.

7 J. Y. Cheng, C. A. Ross, H. I. Smith and E. L. Thomas, *Adv. Mater.*, 2006, **18**, 2505-2521.

8 C. T. Black, R. Ruiz, G. Breyta, J. Y. Cheng, M. E. Colburn, K. W. Guarini, H. C. Kim and Y. Zhang, *IBM J. Res. Dev.*, 2007, **51**, 605-633.

9 X. Deng, J. M. Buriak, P. X. Dai, L. J. Wan and D. Wang, *Chem. Commun.*, 2012, **48**, 9741-9743.

10 K. Naito, H. Hieda, M. Sakurai, Y. Kamata and K. Asakawa, *IEEE Trans. Magn.*, 2002, **38**, 1949-1951.

11 W. I. Park, B. K. You, B. H. Mun, H. K. Seo, J. Y. Lee, S. Hosaka, Y. Yin, C. A. Ross, K. J. Lee and Y. S. Jung, *ACS nano*, 2013, **7**, 2651-2658.

12 K. Choi, S. Nam, Y. Lee, M. Lee, J. Jang, S. J. Kim, Y. J. Jeong, H. Kim, S. Bae, J.-B. Yoo, S. M. Cho, J.-B. Choi, H. K. Chung, J.-H. Ahn, C. E. Park and B. H. Hong, *ACS Nano*, 2015, **9**, 5818-5824.

13 J. Bai, X. Zhong, S. Jiang, Y. Huang and X. Duan, *Nat. Nanotechnol.*, 2010, **5**, 190-194.

14 E. S. Gila, M. Nikhila and M. Indranil, *J. Polym. Sci., Part B: Polym. Phys.*, 2015, **53**, 96-102.

15 C. M. Bates, M. J. Maher, D. W. Janes, C. J. Ellison and C. G. Willson, *Macromolecules*, 2014, **47**, 2-12.

16 S. Y. Kim, J. Gwyther, I. Manners, P. M. Chaikin and R. A. Register, *Adv. Mater.*, 2014, **26**, 791-795.

17 P. Mansky, Y. Liu, E. Huang, T. P. Russell and C. J. Hawker, *Science*, 1997, **275**, 1458-1460.

18 D. Y. Ryu, K. Shin, E. Drockenmuller, C. J. Hawker and T. P. Russell, *Science*, 2005, **308**, 236-239.

19 J. N. Albert, M. J. Baney, C. M. Stafford, J. Y. Kelly and T. H. Epps, *ACS Nano*, 2009, **3**, 3977-3986.

20 M.-L. Wu, J. Li, L.-J. Wan and D. Wang, *Rsc Adv.*, 2014, **4**, 63941-63945.

21 B. H. Kim, K. J. Byeon, J. Y. Kim, J. Kim, H. M. Jin, J. Y. Cho, S. J. Jeong, J. Shin, H. Lee and S. O. Kim, *Small*, 2014, **10**, 4207-4212.

22 D. Ryu, S. Ham, E. Kim, U. Jeong, C. J. Hawker and T. P. Russell, *Macromolecules*, 2009, **42**, 4902-4906.

23 E. Han, K. O. Stuen, Y.-H. La, P. F. Nealey and P. Gopalan, *Macromolecules*, 2008, **41**, 9090-9097.

24 D. Borah, R. Senthamaraikannan, S. Rasappa, B. Kosmala, J. Holmes and M. Morris, *ACS nano*, 2013, **7**, 6583-6596.

25 S. Ham, C. Shin, E. Kim, D. Y. Ryu, U. Jeong, T. P. Russell and C. J. Hawker, *Macromolecules*, 2008, **42**, 6431-6437.

26 B. H. Kim, D. H. Lee, J. Y. Kim, D. O. Shin, H. Y. Jeong, S. Hong, J. M. Yun, C. M. Koo, H. Lee and S. O. Kim, *Adv. Mater.*, 2011, **23**, 5618-5622.

27 J. W. Choi, M. Kim, N. S. Safron, M. S. Arnold and P. Gopalan, *ACS Appl. Mater. Interfaces*, 2014, **6**, 9442-9448.

28 K. S. Novoselov, A. K. Geim, S. V. Morozov, D. Jiang, Y. Zhang, S. V. Dubonos, I. V. Grigorieva and A. A. Firsov, *Science*, 2004, **306**, 666-669.

29 B. H. Kim, J. Y. Kim, S.-J. Jeong, J. O. Hwang, D. H. Lee, D. O. Shin, S.-Y. Choi and S. O. Kim, *ACS Nano*, 2010, **4**, 5464-5470.

30 J. Rafiee, X. Mi, H. Gullapalli, A. V. Thomas, F. Yavari, Y. Shi, P. M. Ajayan and N. A. Koratkar, *Nat. Mater.*, 2012, **11**, 217-222.

31 C.-J. Shih, Q. H. Wang, S. Lin, K.-C. Park, Z. Jin, M. S. Strano and D. Blankschtein, *Phys. Rev. Lett.*, 2012, **109**, 176101.

32 S. Wang, Y. Zhang, N. Abidi and L. Cabrales, *Langmuir*, 2009, **25**, 11078-11081.

33 J. Li, H. Ji, X. Zhang, X. Wang, Z. Jin, D. Wang and L.-J. Wan, *Chem. Commun.*, 2014, **50**, 11012-11015.

34 K. S. Kim, Y. Zhao, H. Jang, S. Y. Lee, J. M. Kim, K. S. Kim, J. H. Ahn, P. Kim, J. Y. Choi and B. H. Hong, *Nature*, 2009, **457**, 706-710.

Table of Contents:
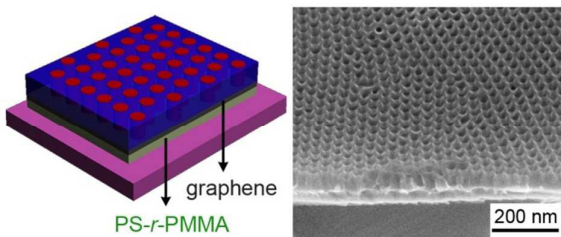
A substrate-independent method to control the orientation of PS-*b*-PMMA film is presented by utilizing monolayer graphene coated PS-*r*-PMMA copolymer layer.